Intravenously administered nanoparticles increase survival following blast trauma

Margaret M. Lashof-Sullivan[a], Erin Shoffstall[a], Kristyn T. Atkins[a], Nickolas Keane[b], Cynthia Bir[b], Pamela VandeVord[c], and Erin B. Lavik[a,1]

[a]Department of Biomedical Engineering, Case Western Reserve University, Cleveland, OH 44106; [b]Department of Biomedical Engineering, Wayne State University, Detroit, MI 48201; and [c]School of Biomedical Engineering and Sciences, Virginia Polytechnic Institute and State University, Blacksburg, VA 24061

Edited by Robert Langer, Massachusetts Institute of Technology, Cambridge, MA, and approved May 30, 2014 (received for review April 16, 2014)

Explosions account for 79% of combat-related injuries, leading to multiorgan hemorrhage and uncontrolled bleeding. Uncontrolled bleeding is the leading cause of death in battlefield traumas as well as in civilian life. We need to stop the bleeding quickly to save lives, but, shockingly, there are no treatments to stop internal bleeding. A therapy that halts bleeding in a site-specific manner and is safe, stable at room temperature, and easily administered is critical for the advancement of trauma care. To address this need, we have developed hemostatic nanoparticles that are administered intravenously. When tested in a model of blast trauma with multiorgan hemorrhaging, i.v. administration of the hemostatic nanoparticles led to a significant improvement in survival over the short term (1 h postblast). No complications from this treatment were apparent out to 3 wk. This work demonstrates that these particles have the potential to save lives and fundamentally change trauma care.

polytrauma | synthetic platelets | lung | clot | medic

On the battlefield, hemorrhage is a leading cause of preventable death (1). Blast injuries account for 79% of combat-related injuries and the majority of cases of traumatic brain injury (2). There are three classifications of blast injury: primary, secondary, and tertiary. Primary blast injuries refer to the direct effects of the overpressure wave, whereas secondary and tertiary insults result from objects propelled by the blast wind and the individual being thrown against other objects, respectively. Owing to the rapid change in pressure, blast traumas can involve hemorrhage in multiple organs, particularly the air-filled organs, brain, and spinal cord.

Blast trauma is unique and difficult to treat because it can damage multiple organs and cause significant hemorrhaging. The shocking reality is that there are no treatments for internal bleeding, although early intervention is essential to minimizing the mortality associated with severe trauma (3). Uncontrolled bleeding is no less lethal beyond the battlefield, being the leading cause of death for civilians age 5–44 y (4, 5).

We need a therapy that can be administered in the field to stop internal bleeding. This therapy must be extremely safe, stable at room temperature, and easily administered. Various therapies, ranging from platelets to recombinant factors to microparticles and nanoparticles, have been considered to date. Administration of allogeneic platelets confers a significant survival advantage in patients with massive trauma, but these platelets have a short shelf life, and administration can cause graft-versus-host disease, alloimmunization, and transfusion-associated lung injuries (6–8). These problems motivated the development of platelet substitutes. Typically, these nanoparticles and microparticles take advantage of the clotting cascade through peptide binding to receptors on activated platelets such as the glycoprotein IIb/IIIa receptor, which can bind fibrinogen, Arg-Gly-Asp (RGD), and dodecapeptide-H12 (HHLGGAKQAGDV). Early designs included RGD-conjugated red blood cells, which were effective in vitro and fibrinogen-coated albumin microparticles, which significantly reduced bleeding time and volume in thrombocytopenic rabbits (9, 10). Platelet-derived particles showed promising results in vitro and in thrombocytopenic rabbits, but did not significantly reduce prolonged bleeding times in thrombocytopenic primates (11, 12). Liposomal nanoparticles are also a potential synthetic core for particles, and particles decorated with RGD and the von Willebrand factor-binding peptide VBP promoted platelet aggregation in vivo and reduced bleeding time in a mouse tail bleeding model (13). Similarly, liposomes carrying the fibrinogen γ chain dodecapeptide (HHLGGAKQAGDV) (14, 15) were effective in thrombocytopenic rats, but might not be effective in healthy models.

In addition to the platelet mimics, recombinant factor 7 (rFVIIa; NovoSeven) has been used to augment hemostasis by supplementing the coagulation cascade. Although rFVIIa can control or reduce massive bleeding in trauma patients, immunogenic and thromboembolic complications are unavoidable risks (16, 17). Nevertheless, rFVIIa is used in the clinic in trauma and surgical situations when bleeding cannot be controlled through other means (16). The data on rFVIIa's efficacy is variable, and it is very expensive; a single dose costs approximately $10,000, and multiple doses are typically needed to impact hemostasis (16). We need an effective, safe therapy for the field.

To address this need, we have developed hemostatic nanoparticles that can halt bleeding when delivered intravenously (18–20). We hypothesized that administration of these hemostatic nanoparticles could increase short-term and long-term survival following blast trauma. We developed a full-body blast model that replicates the injuries seen in personnel exposed to explosions, and tested the effects of administration of hemostatic nanoparticles, control nanoparticles, saline, and rFVIIa on survival, hemorrhaging, and behavioral outcomes following blast trauma.

Results

Development of the Blast Trauma Model. We investigated an 8-msec duration of blast overpressures of 15, 20, and 25 psi to determine the most appropriate blast pressure for modeling blast damage and lethality in mice. Pairs of animals were secured in the prone

Significance

We have developed hemostatic nanoparticles that reduce bleeding and increase survival in both the short term and long term following the complex injuries sustained during blast trauma. This treatment has the potential to be deployed by first responders to save lives.

Author contributions: M.M.L.-S., C.B., P.V., and E.B.L. designed research; M.M.L.-S., E.S., K.T.A., N.K., and P.V. performed research; M.M.L.-S., K.T.A., P.V., and E.B.L. analyzed data; and M.M.L.-S., P.V., and E.B.L. wrote the paper.

Conflict of interest statement: E.B.L. is an inventor listed on patents related to this technology.

This article is a PNAS Direct Submission.

[1]To whom correspondence should be addressed. E-mail: erin.lavik@case.edu.

This article contains supporting information online at www.pnas.org/lookup/suppl/doi:10.1073/pnas.1406979111/-/DCSupplemental.

position in a mesh harness attached to a movable frame directly in line with the main blasting chamber and then exposed to blast overpressure (Fig. 1 *A* and *B*). After exposure, animals were monitored for 1 h to determine the lethality at different pressures. As expected, increasing the pressure of the blast increased the lethality. In this preliminary study, 100% of the untreated mice blasted at 15 psi survived, compared with 60% of those blasted at 20 psi and only 10% of those blasted at 25 psi (Fig. 1*C*).

After the mice were exposed to the primary blast wave, secondary winds caused movement of the harness, resulting in tertiary blast trauma. Examination of the gross anatomy of the organs following injury revealed extensive injury to the thoracic and abdominal regions. Organs including the liver, kidneys, and lungs exhibited damage ranging from slight tears in the tissue to diffuse and severe hemorrhaging and contusions. Lung and liver contusions were observed most often, whereas the gastrointestinal (GI) tract was intact with no abnormalities (Fig. 1 *D* and *E*).

The injuries to the lungs were quantified histologically using eosin staining for red blood cells (Figs. S1 and S2). The degree of lung injury was significantly increased at 20 and 25 psi. This closely correlated with the oxygen saturation levels in these animals, which were significantly lower than those in the animals in the sham-treated and 15-psi groups (Fig. S1*D*). The extensive lung injuries and lower oxygen saturation are consistent with the clinical presentation following blast trauma.

Our model is a complicated model that is sensitive to both primary and tertiary events, making the interactions in the harness critical to the extent of injury. This can be challenging from a scientific standpoint, but these injuries closely model what is seen in patients following blast trauma. Based on the CONWEP software,

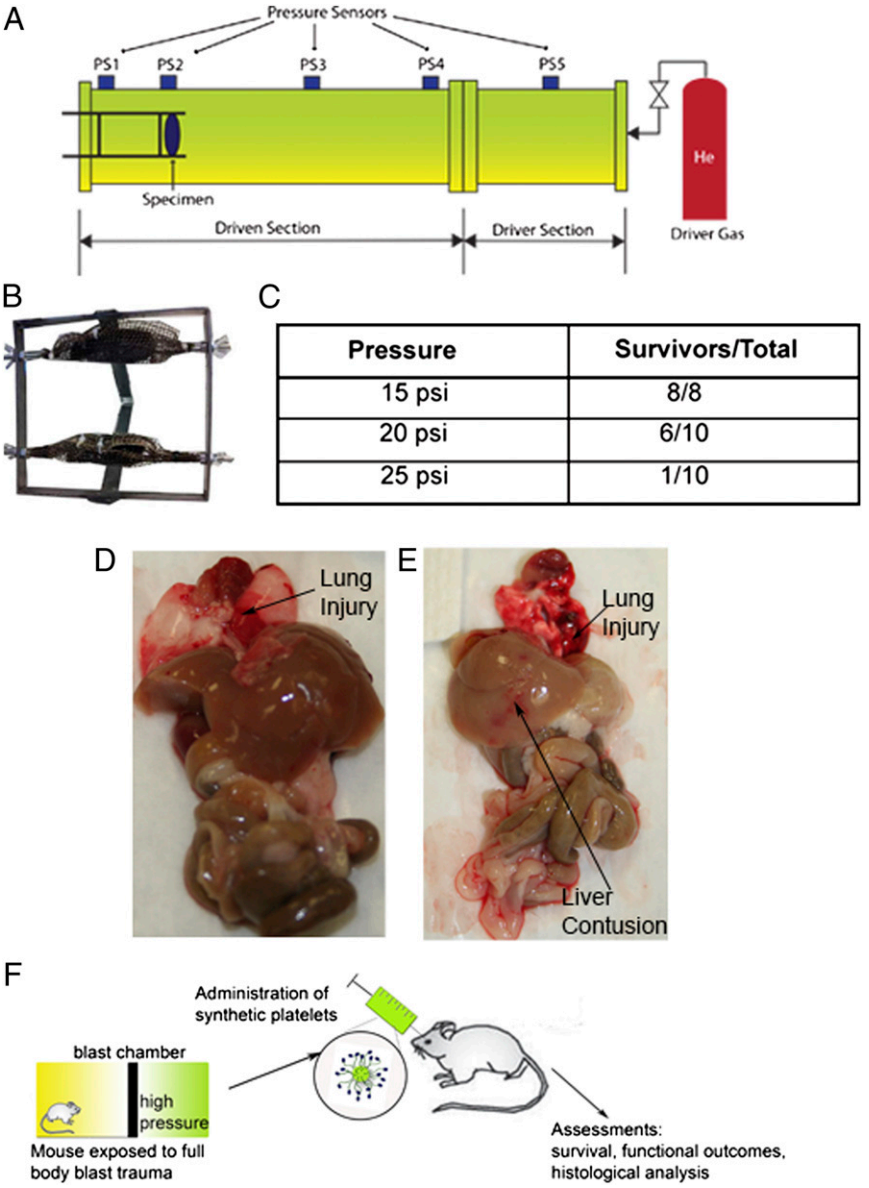

Fig. 1. Development of the blast model and testing paradigm. (*A*) Schematic of the blast tube setup. (*B*) Mice are held in a harness that is on a mobile frame to reduce the degree of tertiary blast injury from the animals striking the harness. (*C*) The fraction of animals that survive at each pressure tested showing that 20 psi led to 60% survival, and 25 psi led to 10% survival. (*D*) Gross examination of organs from 20 psi indicates significant lung injury along with small hemorrhages in the other major organs. (*E*) Gross examination of the organs at 25 psi shows far more extensive hemorrhaging in all of the organs. (*F*) Schematic of the blast experiment. Immediately following the blast trauma, the particles are administered i.v. by retro-orbital injection.

20 psi would be the equivalent of standing 5 m away from a 10-kg TNT equivalence or 10 m away from a 80-kg TNT equivalence. However, no mathematical models available take into account the differences in structure between mice and humans; information from these models must be considered in context, and the clinical presentations in the animal model can provide a more applicable understanding.

Investigating the Role of Hemostatic Nanoparticles on Lethality Following Blast Trauma. Based on the extensive hemorrhaging and 40% lethality, we assessed the capability of the hemostatic nanoparticles to halt internal bleeding at 20 psi. We fabricated and characterized our hemostatic nanoparticles (Fig. 2) and administered them i.v. via retro-orbital injections following the 20-psi blast trauma (Fig. 1*F*). We began our study by examining dosing and investigating the addition of poly(acrylic acid) (PAA) as a flocculating agent on the survival after injury (Fig. S3). PAA is used during nanoparticle synthesis to enable easy collection and subsequent resuspension of particles, and also has been implicated as an anticoagulant (21). In our small-scale study, we found that particles with PAA were at least as effective as particles made without PAA at reducing lethality, and thus we used

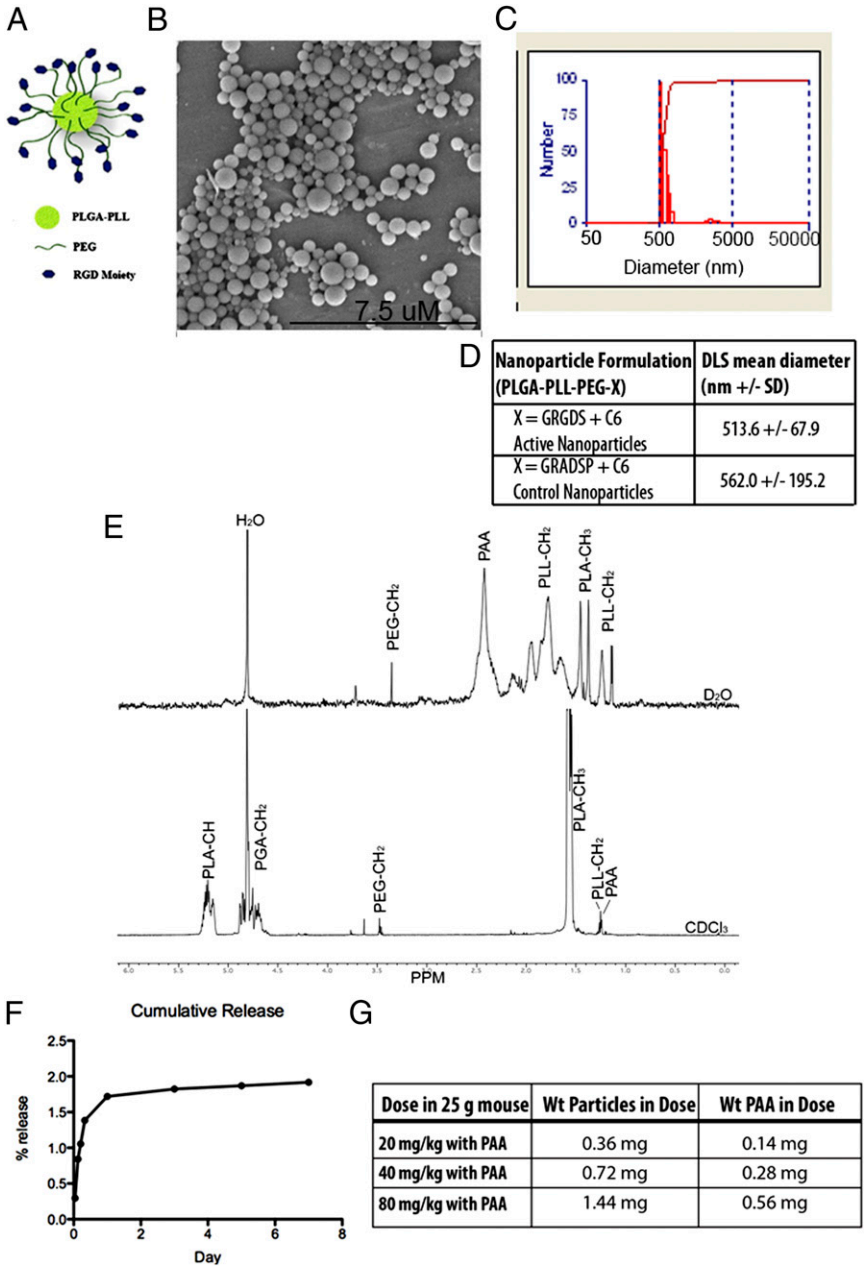

Fig. 2. Characterization of hemostatic nanoparticles. (*A*) Schematic of particle design. (*B*) Scanning electron micrograph of hemostatic nanoparticles showing size range and spherical geometry. (*C*) DLS histogram of particles shown in the scanning electron micrograph. (*D*) Table summarizing DLS data for hemostatic nanoparticles and control nanoparticles loaded with coumarin 6 (C6) with an average hydrodynamic diameter of 500–550 nm. (*E*) NMR of hemostatic nanoparticles showing the PEG content in both deuterated chloroform and deuterated water. The enrichment of PEG in the deuterated water demonstrates that the PEG in the hemostatic nanoparticles have PEG at the surfaces of the particles. (*F*) Release curve for C6 from the hemostatic nanoparticles showing that <1% of the C6 is released over the first week after administration. Error bars denote SEM. (*G*) Formulations of treatments containing PAA.

PAA in all subsequent work. We tested doses of 20 mg/kg, 40 mg/kg, and 80 mg/kg, and found that 40 mg/kg led to the greatest increase in survival, so we focused on this concentration in the subsequent work.

Administration of the hemostatic nanoparticles significantly improved survival following a 20-psi blast (Fig. 3*A*), increasing survival to 95% compared with 60% survival with no treatment [odds ratio (OR), 13; 95% confidence interval (CI), 1.2–143]. There was no significance difference between any other groups (hemostatic nanoparticles vs. lactated Ringer's solution: OR, 8.5; 95% CI, 0.76–100; hemostatic nanoparticles vs. control nanoparticles: OR, 7.1; 95% CI, 0.8–66.7; hemostatic nanoparticles vs. rFVIIa: OR, 5.5; 95% CI, 0.5–58.8). The immediate treatment of blast injury with any fluid replacement appeared to have an effect on the outcome, although we did not find statistical significance. Fluid replacement for blast victims is already standard care because it maintains blood pressure and circulation to the major organs, although it can also exacerbate bleeding (22, 23).

Small cohorts of animals in the nanoparticle groups were maintained as survival groups to 1 wk and 3 wk after the blast injury to examine the long-term effects of nanoparticles, with the remaining animals killed at the 1-h time point (Fig. 2*B*). One of the concerns with hemostatic nanoparticles is whether over time they may cause complications through degradation, clotting, or embolism. Importantly, the vast majority of animals that survived to 1 h lived to the end of the 3-wk study. No complications from the hemostatic nanoparticles were seen, and lethality differences were not statistically different between the 1-wk and 3-wk groups (1 wk, $P = 0.476$; 3 wk, $P = 0.387$). In both groups, a small number of animals died after the 1-h time point. In all cases, the animals that did not survive long term were those that did not initially recover well from the blast and never fully regained mobility and activity.

Role of Hemostatic Nanoparticles on Lung Injury Following Blast Trauma. Histological analysis of the lungs in the control and treatment groups demonstrated a trend toward reduced levels of lung injury in the animals treated with hemostatic nanoparticles that survived to the 1-h time point. As shown in Fig. 4, the 40-mg/kg dose was associated with lower levels of lung injury compared with the control nanoparticle and rFVIIa groups, which is a current clinical treatment for hemorrhage; however, the difference in trends was not statistically significant between the groups. We also analyzed the lung damage in animals that died, although those groups had very few animals ($n = 11$ total animals), and found no significant difference between these groups.

Biodistribution is used as an indicator of particle targeting and to predict how particles are cleared. We found that 9.3% of the injected dose of the hemostatic nanoparticles was recovered at 1 h, which is consistent with the clearance seen in our previous work (18, 20). The majority of the particles (5.2% for hemostatic nanoparticles and 4.7% for control nanoparticles) were found in the lungs, a major site of bleeding for this type of injury (Fig. S4). A large portion of the recovered dose also was found in the liver, suggesting a likely method of clearance. Only a small proportion of the dose was found in the other organs tested (<3%) (Fig. S4).

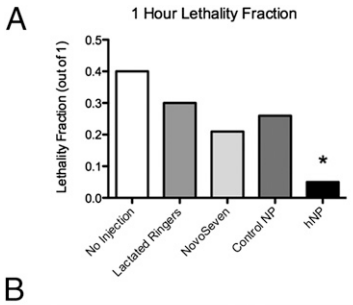

B

Group	Fraction Survival at 1 week post blast	Fraction Survival at 3 weeks post blast
hNP	10/11	6/7
Control NP	8/10	5/7

Fig. 3. Lethality from blast injury is significantly reduced by the administration of the hemostatic nanoparticles. (*A*) Administration of the hemostatic nanoparticles increased survival at 1 h to 95% ($n = 21$), compared with 60% survival with no treatment ($n = 10$) (OR, 13; 95% CI, 1.2–143). There was no significant difference between any other groups. (*B*) A small group of animals that survived to 1 h were maintained to 1 wk and 3 wk. The majority of these animals survived without any apparent complications from treatment. Lethality differences were not statistically significant (1 wk, $P = 0.476$; 3 wk, $P = 0.387$).

Discussion

Blast trauma in humans can cause a broad range of injuries, including traumatic brain injury, lung injury, blunt trauma, and penetrating ballistic trauma, with many levels of severity and mortality of 8–25% (22). Modeling blast injury in a repeatable and representative manner is a significant challenge. The degree of injury suffered depends on many factors, including the blast peak overpressure, proximity and orientation of the body to the blast wave, and number of overpressure peaks, among others (22). We found that a 20-psi overpressure resulted in injuries that are most representative of damage to the lungs and other organs, including the liver and GI tract, in a primary blast injury (24). The animals also moved against the harness during the blasts, leading to tertiary injuries, which are very common in blast victims (25). The 25-psi blast resulted in injuries beyond what is likely survivable, with extensive damage to all organs. In fact, we tested the administration of hemostatic nanoparticles following the 25-psi blast and saw no benefit to this therapy (Fig. S5). Hemostatic nanoparticle therapy has the greatest impact in cases of where bleeding is extensive but organ damage is not too severe.

Nonetheless, treatment with the hemostatic nanoparticles did confer a clear improvement in survival. The hemostatic nanoparticle group demonstrated a trend toward less lung damage. Lung injury induced by primary blast overpressure is known to result in increased red blood cells and edema within the vessels and alveoli of the lungs (24). A rise in pressure as the blast wave creates compression and shearing against the thoracic wall ruptures capillary walls and forces blood through the alveolar septa, ultimately causing hemorrhage and interstitial edema in the lungs. The activated nanoparticles are designed to augment primary hemostasis. Histological analysis of lung tissue in animals treated with our particles showed an encouraging outcome, suggesting that survival and lung damage are correlated and that our particles may reduce bleeding into the lungs, aiding survival.

One of the main concerns in the present study was the presence of any adverse long-term effects of nanoparticle administration. Although a few animals died over the longer time periods (1 wk and 3 wk), none exhibited any evident complications resulting from the nanoparticle treatment, such as gasping, stroke, or apparent blocked vessels. The one animal from the hemostatic nanoparticle group that died was euthanized at 1 d postinjury when it appeared to be very weak. Two animals from the control nanoparticle group died before the 3-wk time point. Although only a small number of animals were maintained over the long term, our data strongly suggest that the particles can be administered safely without any apparent short-term or long-term side effects. This is an important consideration in the clinical translation of this technology.

Ultimately, the administration of hemostatic nanoparticles significantly reduced lethality compared with untreated controls following blast trauma and produced no apparent complications.

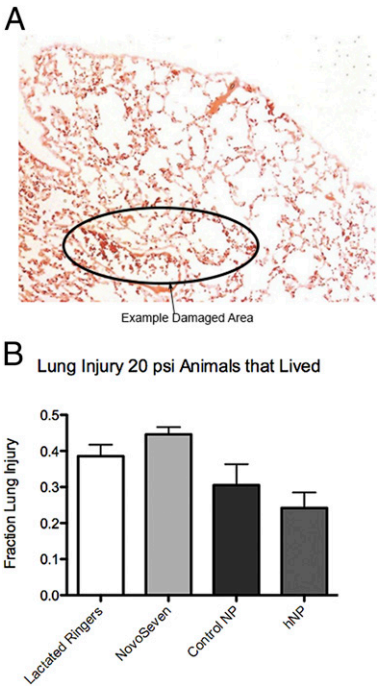

Fig. 4. Lung injury following blast trauma. (*A*) Representative image of lungs damaged at 20 psi showing the large quantity of red blood cells in the lungs. (*B*) Quantification of lung injury in the groups at 20 psi. There is a trend toward reduced injury in the hemostatic nanoparticle group, but the differences are not significant. Error bars denote SEM.

Our model suggests that these nanoparticles may be a powerful front- line therapy for blast trauma.

Materials and Methods

Experimental Design. Our first step in the experimental design was to determine the degree of lethality with respect to overpressure in our blast model. Based on previous experience with blast trauma, we performed a pilot study with eight animals per group (only six animals were used for the 15-psi blast, because all survived) to determine the pressure that led to hemorrhaging and 50% lethality. We found that 20 psi was optimal based on these considerations.

We blocked each round of testing and performed all of the treatments during each round of testing. The person performing the blast testing and monitoring the animals was blinded to the treatment, as were all of the team members who maintained animals after the experiment and performed histological assessments.

An animal was excluded from the analysis if the video of the blast showed that the harness was loose or the animal hit its head on the screws holding the apparatus. Animals were not excluded for any other reason. We anticipated needing 15–20 animals per group based on a power analysis. The experiments were halted when significance was determined.

Materials. Poly(lactic-*co*-glycolic) acid (PLGA) (Resomer 503H) was purchased from Evonik Industries. Poly-l-lysine (PLL) and poly(ethylene glycol) (PEG) (~4,600 Da) were purchased from Sigma-Aldrich. All reagents were ACS grade and were purchased from Thermo Fisher Scientific. PLGA-PLL-PEG block copolymer was created using standard bioconjugation techniques as described previously (26).

Particle Synthesis. PLGA-PLL-PEG-GRGDS block copolymer for the hemostatic nanoparticles and PLGA-PLL-PEG-GRADSP were synthesized using protocols described previously (18–20). In brief, the triblock polymer was synthesized using stepwise conjugate reactions. The PLGA was coupled to poly(ε-cbz-L-lysine) (PLL-cbz; PLL with carbobenzoxy-protected amine side groups). The conjugation was confirmed by UV-vis spectroscopy. After the PGA-PLL-cbz was deprotected with HBr, the free amines of the PLL-NH3 were reacted with CDI-activated PEG in a 5:1 molar excess (27).

The GRGDS was conjugated to PEG-PLGA (or the conservatively substituted GRADSP) as described previously (20). In brief, the peptide was conjugated by dissolving the PLGA-PLL-PEG (1 g) in anhydrous DMSO to a concentration of 100 mg/mL and the oligopeptide (25 mg) was dissolved in 1 mL of DMSO and added to the stirring polymer solution. The free amine of the oligopeptide then reacted with free end of the CDI-activated PEG. The mixture reacted to 3 h, and was then transferred to dialysis tubing (SpectraPor, 2 kFa molecular weight cutoff) and dialyzed for 4 h before being snap-frozen in liquid nitrogen and lyophilized (20).

To form particles, the polymer was dissolved at a concentration of 20 mg/mL in acetonitrile containing coumarin-6 (C6), a fluorescent dye used to track the particles after injection (loaded at 1% wt/wt). This dye has been previously shown to release <0.5% of the initial loading by 24 h and 1.5% by 7 d. This solution was added dropwise to a volume of stirring PBS twice that of the acetonitrile (28). Precipitated nanoparticles form as the water-miscible solvent is displaced.

Coacervate Precipitation. The method for nanoparticle collection was adapted from D'Addio et al. (29). In brief, one mass equivalent of dry PAA (Sigma-Aldrich; molecular weight 1,800) was added to the stirring particle suspension. Then 1% (wt/vol) PAA was added to the stirring suspension until flocculation occurred, at ~10 mL. The flocculated particles were collected by centrifugation at 500 × *g* and rinsed three times with 1% PAA (with centrifugation at 250 × *g* at 4 °C for 2 min between rinses). After the final rinse, particles were resuspended to ~10 mg/mL with deionized water, snap-frozen in liquid nitrogen, and lyophilized. Particles were resuspended in lactated Ringer's solution before use.

Characterization. Nanoparticles were characterized for size and polydispersity using dynamic light scattering (DLS) (90Plus; Brookhaven Instruments) and scanning electron microscopy (Hitachi S4500). DLS data were represented as the effective diameter as calculated using the 90Plus software. The PEG corona of the nanoparticles was characterized by NMR (600-MHz Varian Inova NMR spectrometer). Data were collected with particles suspended in deuterated water and again with particles dissolved in deuterated chloroform.

Blast Trauma Injury. Male C57BL/6 mice (9-10 wk old; Harlan Labs) were used in this study. The mice were allowed to acclimate for a period of three days before testing. They were handled by researchers to help diminish fear, and were given food and water ad libitum while being cycled on a 12-h light/dark schedule. Approval for all experiments was obtained from the Wayne State University's Institutional Animal Care and Use Committee before testing. A custom-built 0.3 m diameter shock tube located at Wayne State University Bioengineering Center was used to induce blast overpressure. Mylar sheets (GE Richards Graphic Supplies) were placed between the compression chamber (driver) and the testing chamber (driven) to attain peak pressures. Pressure sensors (Free-Field ICP Blast Pressure Sensor 137A22; PCB Piezotronics) were placed within the driver and driven sections to accurately measure the static overpressure within the tube. An additional pressure sensor was placed on the platform holding the mice to most accurately determine the level of static overpressure the mice were exposed to. A portable analog-to-digital data acquisition system (DASH 8HF; Astro-Med) collected the data from all pressure transducers at 250 kHz per channel.

Before blast exposure, two mice were anesthetized with a ketamine/xylazine solution and their weights recorded. After being monitored for 10 min postinjection of anesthetics they were placed in a custom-built restraint harness and exposed to a whole-body blast. Animals were exposed to a single shock wave with an intensity of 0, 15, 20, or 25 psi for an 8-msec positive phase duration.

Administration of Particles Following Blast Trauma. After the blast exposure, animals were immediately removed, placed on a heating pad, and monitored for a 1-h evaluation period. Within 5 min of the blast, the treatments (hemostatic nanoparticles, 50 μL of a 20 mg/mL solution in lactated Ringer's; control nanoparticles, 50 μL of a 20 mg/mL solution in lactated Ringer's; rFVIIa, 50 μL; lactated Ringer's, 50 μL; or no treatment) were administered retro-orbitally.

If the animal died before the 1-h assessment, the organs (lungs, kidneys, spleen, liver, GI, and brain) were quickly harvested for histological analysis. On survival to the 1-h time point, the animal was killed by transcardial perfusion of cold saline (0.9% sodium chloride) followed by fixative solution containing 4% paraformaldehyde. Brains were dehydrated in a solution containing 15% sucrose for 24 h before being fixed in paraformaldehyde solution. Tissues were kept for histological assessment, and some organs were acquired for biodistribution. A small cohort of animals was sustained for up to

3 wk postinjury to evaluate both a correlation between survival in the acute phase and long-term survival, as well as any complications associated with administration of hemostatic nanoparticles or control nanoparticles.

Statistics for Lethality Study. The persons performing the blast trauma and administering the treatment in this study were blinded to the treatments. Another individual also blinded to the treatment independently recorded death. Survival was analyzed by binomial logistic regression with Wald χ^2 tests between ORs (SAS).

Characterization of Lung Injury Following Blast Trauma. Forty-eight hours after fixation, the lungs were placed in OCT embedding medium and allowed to freeze on dry ice. The tissues were then cut and stained with hematoxylin and eosin (H&E) or eosin only. Eosin-only sections were used to quantify lung injury. Images were taken of three regions of interest in each lung tissue section. Using ImageJ software, the images were converted to grayscale, and optical density readings were collected to determine the level of hemorrhaging in the lung tissue. Fig. S3 shows how each section was analyzed. After the percent of injured area was calculated, significance was determined and error was reported as mean ± SD. Histological statistical analysis was calculated with two-way ANOVA, followed by a post hoc LSD test. Significance was indicated by $P < 0.05$.

Biodistribution of Particles Following Blast Trauma. Biodistribution was performed using protocols described previously (19). In brief, major organs (liver, kidneys, heart, spleen, lungs, and brain) were harvested and lyophilized for the biodistribution assay performed on the HPLC. The dry weight of the whole organ was recorded and 100–200 mg of dry tissue was homogenized (Precellys 24) and incubated overnight in acetonitrile at 37 °C. This dissolved any nanoparticles present in the tissue and left the C6 in the organic solvent solution. Tubes were then centrifuged at 15,000 × *g* for 10 min to remove solid matter and supernatant was tested on the HPLC. Mobile phase was 80% acetonitrile and 20% aqueous (8% acetic acid). Stationary phase was a Waters Symmetry C18 column (100 Å, 5 μm, 3.9 mm × 150 mm). Samples that oversaturated on the fluorescence detector (450/490 nm ex/em) were diluted and rerun. Based on the known C6 loading and injection volume of particles, data are represented as the percentage of particles injected in each organ.

ACKNOWLEDGMENTS. This work was funded by US Department of Defense Grant W81XWH-11-2-0014 and National Institutes of Health Director's New Innovator Award DP20D007338. The content is solely the responsibility of the authors and does not necessarily represent the official views of the Office of the Director, National Institutes of Health, or the National Institutes of Health.

1. Champion HR, Bellamy RF, Roberts CP, Leppaniemi A (2003) A profile of combat injury. *J Trauma* 54(5, Suppl):S13–S19.
2. Krug EG, Sharma GK, Lozano R (2000) The global burden of injuries. *Am J Public Health* 90(4):523–526.
3. Regel G, Stalp M, Lehmann U, Seekamp A (1997) Prehospital care, importance of early intervention on outcome. *Acta Anaesthesiol Scand Suppl* 110:71–76.
4. Eastridge BJ, et al. (2012) Death on the battlefield (2001-2011): Implications for the future of combat casualty care. *J Trauma Acute Care Surg* 73(6, Suppl 5):S431–S437.
5. Warden D (2006) Military TBI during the Iraq and Afghanistan wars. *J Head Trauma Rehabil* 21(5):398–402.
6. Kauvar DS, Lefering R, Wade CE (2006) Impact of hemorrhage on trauma outcome: An overview of epidemiology, clinical presentations, and therapeutic considerations. *J Trauma* 60(6, Suppl):S3–S11.
7. Malone DL, et al. (2003) Blood transfusion, independent of shock severity, is associated with worse outcome in trauma. *J Trauma* 54(5):898–905.
8. Ketchum L, Hess JR, Hiippala S (2006) Indications for early fresh-frozen plasma, cryoprecipitate, and platelet transfusion in trauma. *J Trauma* 60(6, Suppl):S51–S58.
9. Coller BS, et al. (1992) Thromboerythrocytes: In vitro studies of a potential autologous, semi-artificial alternative to platelet transfusions. *J Clin Invest* 89(2):546–555.
10. Levi M, et al. (1999) Fibrinogen-coated albumin microcapsules reduce bleeding in severely thrombocytopenic rabbits. *Nat Med* 5(1):107–111.
11. Fitzpatrick G, Vibhudatta A, Agashe H, Dee J (2010) Trehalose-stabilized freeze- dried human platelets, Thrombosomes, reduce blood loss in thrombocytopenic rabbit ear bleed model by as much as 89.5%. *Vox Sang* 99(Suppl 1):261.
12. Fitzpatrick GM, Cliff R, Tandon N (2013) Thrombosomes: A platelet-derived hemostatic agent for control of noncompressible hemorrhage. *Transfusion* 53(Suppl 1): 100S–106S.
13. Modery-Pawlowski CL, Tian LL, Ravikumar M, Wong TL, Sen Gupta A (2013) In vitro and in vivo hemostatic capabilities of a functionally integrated platelet-mimetic liposomal nanoconstruct. *Biomaterials* 34(12):3031–3041.
14. Okamura Y, et al. (2005) Hemostatic effects of phospholipid vesicles carrying fibrinogen gamma chain dodecapeptide in vitro and in vivo. *Bioconjug Chem* 16(6): 1589–1596.
15. Okamura Y, et al. (2010) Visualization of liposomes carrying fibrinogen gamma-chain dodecapeptide accumulated to sites of vascular injury using computed tomography. *Nanomedicine (Lond Print)* 6(2):391–396.
16. Benharash P, Bongard F, Putnam B (2005) Use of recombinant factor VIIa for adjunctive hemorrhage control in trauma and surgical patients. *Am Surg* 71(9):776–780.
17. Martinowitz U, Zaarur M, Yaron BL, Blumenfeld A, Martonovits G (2004) Treating traumatic bleeding in a combat setting: Possible role of recombinant activated factor VII. *Mil Med* 169(12, Suppl):16-8, 4.
18. Bertram JP, et al. (2009) Intravenous hemostat: Nanotechnology to halt bleeding. *Sci Transl Med* 1(11):11ra22.
19. Shoffstall AJ, et al. (2012) Intravenous hemostatic nanoparticles increase survival following blunt trauma injury. *Biomacromolecules* 13(11):3850–3857.
20. Shoffstall AJ, et al. (2013) Tuning ligand density on intravenous hemostatic nanoparticles dramatically increases survival following blunt trauma. *Biomacromolecules* 14(8):2790–2797.
21. Monien BH, Cheang KI, Desai UR (2005) Mechanism of poly(acrylic acid) acceleration of antithrombin inhibition of thrombin: Implications for the design of novel heparin mimics. *J Med Chem* 48(16):5360–5368.
22. Mayorga MA (1997) The pathology of primary blast overpressure injury. *Toxicology* 121(1):17–28.
23. DePalma RG, Burris DG, Champion HR, Hodgson MJ (2005) Blast injuries. *N Engl J Med* 352(13):1335–1342.
24. Elsayed NM (1997) Toxicology of blast overpressure. *Toxicology* 121(1):1–15.
25. Wightman JM, Gladish SL (2001) Explosions and blast injuries. *Ann Emerg Med* 37(6): 664–678.
26. Bertram JP, et al. (2009) Functionalized poly(lactic-co-glycolic acid) enhances drug delivery and provides chemical moieties for surface engineering while preserving biocompatibility. *Acta Biomater* 5(8):2860–2871.
27. Hermanson G (1996) *Bioconjugate Techniques* (Academic Press, San Diego), pp xxv, 785.
28. Cheng J, et al. (2007) Formulation of functionalized PLGA-PEG nanoparticles for in vivo targeted drug delivery. *Biomaterials* 28(5):869–876.
29. D'Addio SM, et al. (2010) Novel method for concentrating and drying polymeric nanoparticles: Hydrogen bonding coacervate precipitation. *Mol Pharm* 7(2):557–564.